JOURNAL OF CATALYSIS 70, 41–52 (1981)

Infrared and Temperature-Programmed Desorption Study of the Acidic Properties of ZSM-5-Type Zeolites

NAN-YU TOPSØE,* KARSTEN PEDERSEN,* AND ERIC G. DEROUANE†,[1]

* *Haldor Topsoe Research Laboratories, DK-2800-Lyngby, Denmark, and,* † *Facultés Universitaires de Namur, Laboratoire de Catalyse, Rue de Bruxelles 61, B-5000 Namur, Belgium*

Received June 24, 1980; revised December 18, 1980

Infrared spectroscopy and temperature-programmed desorption have been used to investigate the acidic properties of ZSM-5-type zeolites. Active acidic sites, in concentration related to the aluminum content and most probably located at the channel intersections, are characterized by an ir band at 3600 cm^{-1} and a desorption peak near 773 K (γ state). Weaker acidic sites are characterized by an ir band at 3720–3740 cm^{-1} and a desorption peak at about 500 K (β state). They probably correspond to terminal silanol groups on the external surface of the zeolite or possibly nonzeolitic impurities. Lewis acidic sites are also characterized by the γ-state desorption peak, while Na adsorption centers for ammonia give rise to a β-state peak. Pyridine desorption helps dehydroxylation of the zeolite.

INTRODUCTION

Some acidic properties of zeolites of the ZSM-5 family have been reported and discussed in the recent literature (*1–3*). Although some ammonia temperature-programmed-desorption (TPD) data are also available (*4, 5*), the main contribution to the understanding of the acidic properties of H–ZSM-5 (the protonated form of zeolite ZSM-5) has been through the use of infrared (ir) spectroscopy (*1, 3*), electron spin resonance (ESR) (*1*), and microcalorimetry (*2, 3*).

Important conclusions, however, raising fundamental questions, were that ZSM-5 zeolite contains acidic hydroxyls rather similar to those of mordenite (*1*) and that the more acidic hydroxyls (ir band at near 3605 cm^{-1}) were irreversibly removed by dehydration at high temperature (*1*). Pyridine was shown to be unsatisfactory as a probe for Lewis acidity inside the channel structure because of its restricted accessibility to the structural sites, resulting from its size and binding mode to Lewis acidic centers (*1, 3*). However, a combined ir–microcalorimetric study (*3*) of various acidic ZSM-5 zeolites confirmed that the generally assumed stoichiometry for the dehydration of Brønsted (BA) to Lewis (LA) acid sites ($2BA \rightarrow LA + H_2O$) (*6, 7*) was well followed upon progressive dehydroxylation. The maximum heat of ammonia adsorption on H–ZSM-5 was found to be slightly higher than that observed for mordenite (i.e., 36 vs 34 kcal mol^{-1}) when activation was performed at about 800 K, and increased with dehydroxylation temperature (39–40 kcal mol^{-1} after activation at 1070 K). A wide variation in adsorption heat was observed with coverage and diffusional limitations were shown to restrict the access of ammonia to the strongest acidic sites (*2, 3*). Ammonia TPD data (*4, 5*) provided some additional information on the binding mode of ammonia to the acidic sites; four discrete peaks were observed of which the high-temperature one (maximum near 800 K) showed some correlation with Na content and seemed characteristic of acidic ZSM-5.

On the basis of such observations, sev-

[1] To whom queries concerning this paper should be sent.

0021-9517/81/070041-12$02.00/0

eral questions may be raised and some clarifications will be attempted in this paper. The first one concerns the *origins of the two hydroxyl bands* which are observed at 3600–3605 and 3720 cm^{-1}, respectively, as they each have a distinct intensity behavior with respect to varying Si/Al ratios, acidification treatments, and rehydration (*1, 3*). Second, additional information on the *distribution in strength* of the acidic sites is needed since discrete acidic centers were observed by ir and TPD (two by ir and more than two by TPD) in contrast to the near continuum inferred from microcalorimetry data. The third matter is to assess the respective and relative *roles* of these various acidic centers *as catalytic sites*. For instance, it was shown that ethylene reacts preferably with the Brønsted sites characterized by the ir band at 3605 cm^{-1} (*8*).

The threefold aim of the present paper is then to characterize the acidic centers of ZSM-5-type zeolites in terms of their spatial, strength, and catalytic activity distribution patterns.

EXPERIMENTAL

Materials

Zeolites of the ZSM-5 family were synthesized as described previously (*4, 22, 23*). Si/Al ratios for samples HTZ-1 and HTZ-2 were 11.8 and 18.0, respectively. The (Na,H) form of the zeolite (already partially protonated due to the thermal decomposition of the alkylammonium cations) was formed after the precursors were calcined in air (at 820 K for 2 h). The acidic (or protonated) form was obtained by acidic exchange using 0.5 *N* HCl at 353 K for 1 h. The acidic catalyst was further calcined at 823 K for 2 h.

Infrared Spectroscopy

The samples (100 mg) were pressed into self-supporting wafers and placed into a stainless steel *in situ* ir cell allowing heating under vacuum (about 10^{-6} Torr) around 773 K. Pyridine, spectroscopic grade, was dried over an activated Linde 5A molecular sieve and further degassed by the conventional freeze–pump–thaw technique.

Prior to adsorption the samples were evacuated to about 10^{-6} Torr at 723 K for 12 h. The samples were then cooled to 423 K where nearly 1 Torr of pyridine was introduced into the ir cell. After 1 h of adsorption, the excess and weakly adsorbed pyridine was removed by evacuating at the same temperature for 30 min to below 10^{-5} Torr. Presumably only the chemisorbed pyridine remained on the surface. Desorption was then continued by evacuation at progressively higher temperatures and ir spectra were recorded on a Perkin–Elmer 180 spectrometer at the various stages of desorption. Background spectra, i.e., prior to adsorption, have been subtracted from all spectra by a Nicolet signal averager (model 535) such that the effects of adsorption and thermal treatments could be more clearly seen.

Adsorption and Temperature-Programmed Desorption of Ammonia

NH_3 adsorption and TPD was achieved, using the setup schematized in Fig. 1a, on the catalyst *in situ* in the reactor system, following its initial activation at 823 K.

NH_3 in N_2 (0.5%) was used as adsorption gas, while desorption was achieved under a constant flow of pure N_2 (10 liters h^{-1}). The concentration of NH_3 in the exit gas was continuously monitored by using a Leybold Binos 1 infrared analyzer (5000 ppm NH_3, single channel, 200-mm cuvette, and InSb filter).

The catalyst (about 0.5 g) was placed in a quartz reactor and saturated with the ammonia adsorption gas, at which point it was first eluted at 293 K. The total NH_3 uptake was estimated by integration of the C_{NH_3} vs time profile (Fig. 1b). Following elution at 293 K, i.e., when the concentration of NH_3 was lower than 5 ppm,

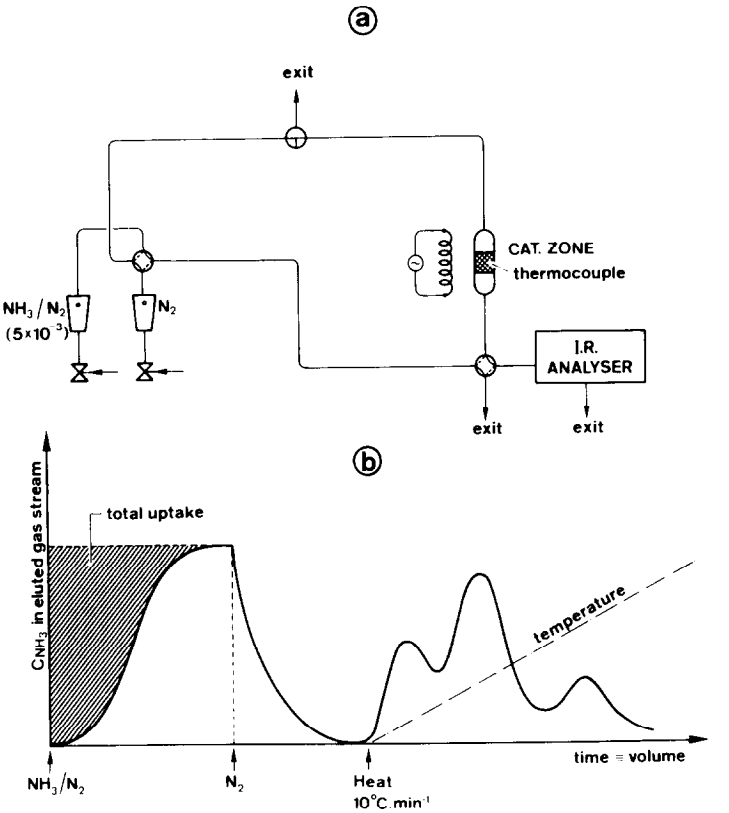

FIG. 1. Ammonia adsorption and temperature-programmed desorption (TPD). (a) Experimental setup; (b) typical (schematic) adsorption and TPD trace.

the temperature of the catalyst was linearly increased at a controlled rate which could be varied (from 5 to 40 min^{-1} in various desorption experiments for the same catalyst) to estimate heats of desorption. The desorbed amount was evaluated by integration of the desorption curve and the difference between the uptake (at room temperature) and desorbed (up to 873 K) amounts was the physisorbed NH_3 that was eluted at 293 K.

RESULTS

Infrared Bands of Structural OH Groups vs Activation Temperature

In close agreement with the previous data (*1*) ir bands in the OH stretching region are observed at 3600, 3660, and 3720 cm^{-1}. Intensity changes of these bands with increasing activation temperature under vacuum for the acidified zeolite HTZ-1 are shown in the difference ir spectra (obtained by subtracting the spectra observed at various activation temperatures from the original spectrum before activation) in Fig. 2. The horizontal straight line represents zero change of band intensities. The band area under this line represents the decrease in intensities, whereas that above the line represents the increase in intensities due to the thermal treatment. The curves show an initial increase in intensity of the OH stretching band at ~3600 cm^{-1}, and a rapid decrease of intensities of the bands around 3000–3500 and ~3680 cm^{-1} with increasing evacuation temperature. At about 473 K, the 3600-cm^{-1} band starts disappearing slowly with still little change in the 3720- to 3740-cm^{-1} band. At temperatures above 673 K, however, one can clearly

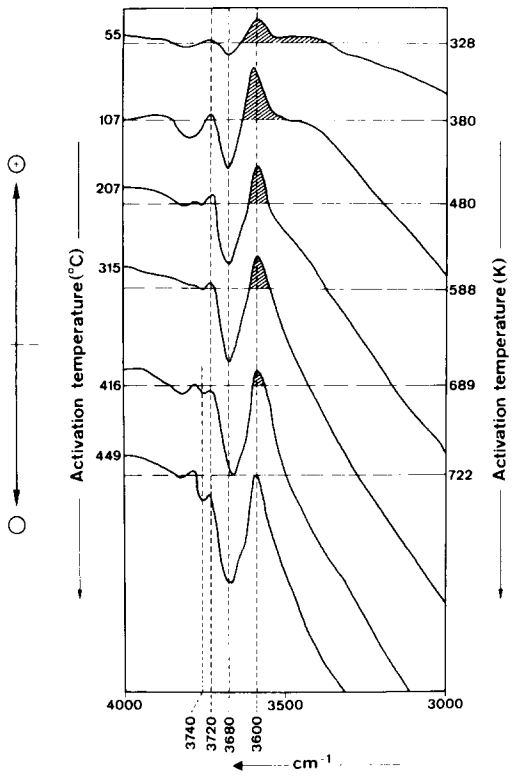

FIG. 2. Difference ir spectra following activation under vacuum at various temperatures of protonated HTZ-1 zeolite.

detect an intensity decrease of the latter band as well.

The dehydration and dehydroxylation can therefore be described as a rapid initial loss of physisorbed water molecules (the 3000- to 3500-cm^{-1} band) in agreement with the hydrophobicity of the zeolite (*22*). Simultaneously, Si–OH–Al groups characterized by the ir band at ~3600 cm^{-1} (*1*) are less perturbed by hydrogen-bonded water molecules and the intensity of this band hence increases with progressive desorption of water up to 423 K. Most water has been removed above this temperature, at which stage the quantity of hydroxyl groups begins to diminish. The Si–OH–Al groups (~3600 cm^{-1}) and the hydroxyl groups at ~3720 cm^{-1} are later shown to be acidic (or more specifically they are Brønsted acid sites) in agreement with previous data (*1*, *3*).

Pyridine Adsorption (ir)

The nature of the acid sites and their relative strengths for HTZ-1 and HTZ-2 zeolites which differ by their Si/Al ratios were studied by means of infrared spectra following pyridine adsorption. Pyridine was adsorbed and then evacuated at 423 K such that only chemisorbed pyridine remained on the zeolites. This eliminates the difficulty caused by overlapping bands of physically adsorbed and hydrogen-bonded pyridine which may obscure the bands due to coordinated pyridine. The bands due to the chemisorbed pyridine are shown in Fig. 3. These occur at 3250, 3165, and 3070 cm^{-1} in the bond stretching region and at ~1600, 1540, 1485, and 1450 cm^{-1} in the bending region. The high-frequency bands are assigned to the N–H stretching vibration of the pyridinium ion. The 1540-cm^{-1} band is attributed to the C–C stretching vibration of the pyridinium ion and is most commonly used for detecting the presence of Brønsted acidity. Lewis acidity, on the other hand, is indicated by the band at 1450 cm^{-1} which arises from the C–C stretch of a coordinatively bonded pyridine complex. The 1485-cm^{-1} band is not as useful for identification since it is common to both species (*9*). Other less well resolved bands at ~3720, ~3660, and ~3500 cm^{-1} are due to OH stretching vibrations.

Figure 3 shows a study of desorption of pyridine as a function of temperatures of evacuation and casts some light on the strength of the various acid sites. It should be noted that these spectra are again difference spectra and show only the differences which arise from the pyridine adsorption and further desorption in that the spectrum of the sample prior to adsorption has been subtracted from all desorption spectra recorded subsequently. Thus, the horizontal line represents as

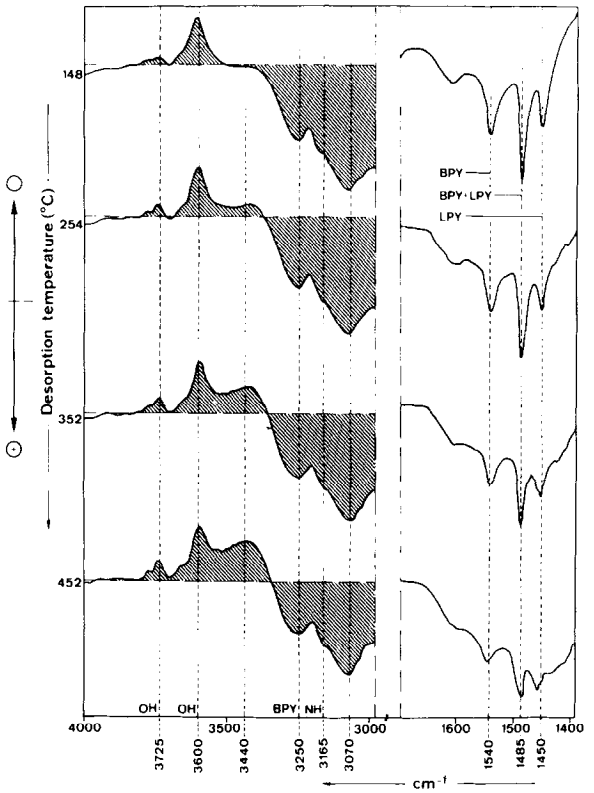

FIG. 3. Difference ir spectra following pyridine adsorption at 323 K and desorption at various temperatures (HTZ-1, protonated ZSM-5-type zeolite).

previously no change in spectra; however, the band contours above the line now are due to species removed from the original sample and those under the line are from the adsorbed species. This manner of data presentation has the advantage that it not only clearly shows the adsorbed species remaining on the surface without interference of an uneven background but also reveals the nature of the desorbed species. It is indeed elucidating to observe the direct relationship of hydroxyl groups and adsorbed pyridinium ions.

Adsorption of pyridine causes a decrease in the intensity of the OH bands at 3725 and 3600 cm^{-1}. As the desorption temperature is progressively increased from 323 to 623 K, it is further seen that the pyridinium ion bands disappear more quickly than those of coordinated pyridine while at the same time (adsorbed) water is being removed (at ~3440 cm^{-1}) as well as some more hydroxyl groups (band at 3725 cm^{-1}). Clearly, the bands at 3600 and 3725 cm^{-1} characterize Brønsted acidic sites.

Figure 4 compares data for zeolites HTZ-1 and HTZ-2. A plot of the absorbance per sample mass (or the acid site population) against the pyridine desorption temperature indicates that the population of probed Brønsted acid sites is higher than that of probed Lewis acid sites for both zeolites, and that the pyridinium ions are removed more rapidly than coordinatively bound pyridine with increasing temperature of desorption. The total Lewis acidity is rather similar for both zeolites, whereas the number of

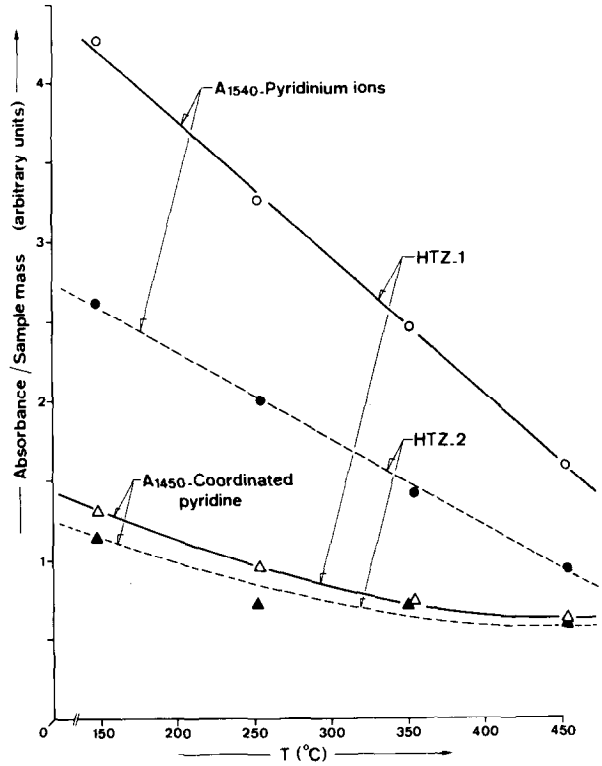

FIG. 4. Brønsted and Lewis acid sites populations (as probed by pyridine) as functions of pyridine desorption temperature for protonated HTZ-1 and HTZ-2 zeolites.

Brønsted acid sites is much higher in HTZ-1 than in HTZ-2 as expected because of its lower Si/Al ratio.

Adsorption and Temperature-Programmed Desorption of Ammonia

Following the elution of physisorbed NH_3 at room temperature, three different states of chemisorbed ammonia are distinguished which show maxima in the desorption rate at 333–373, 423–473, and 593–773 K, respectively, in good agreement with other reports (*4, 5*). These chemisorption states will be referred to in order as α, β, and γ, respectively. Typical TPD patterns are illustrated in Fig. 5 which also shows that the distribution of chemisorbed ammonia on these states depends on catalyst pretreatment and/or deactivation. The β state is missing and the α state is strongly reduced in a catalyst partially deactivated by operating the methanol-to-hydrocarbons reaction at ~645 K (see Table 1). The effect of the latter on the γ state is less drastic. Both the γ and β states may be regenerated partially by progressive heating in dry nitrogen up to 873 K (in a TPD-like experiment), while the α state stays largely poisoned.

Table 1 shows the distribution of ammonia on the α, β, and γ states (for the protonated HTZ-1 catalyst) for a fresh, strongly deactivated, and a partially regenerated (TPD run C follows TPD run B) catalyst. The fact that the amount of physisorbed (reversibly adsorbed at 293 K) NH_3 is drastically reduced once the catalyst is deactivated (by coking) and does not increase upon further partial regeneration further supports the behaviors of the α, β, and γ states as first described.

It may be interesting to observe in ad-

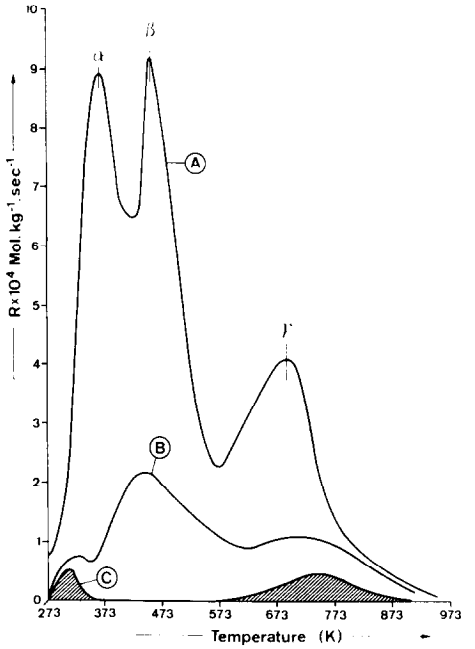

FIG. 5. Temperature-programmed desorption of NH_3 from the protonated HTZ-1 catalyst (sample weight, 0.5 g; heating rate, 10 K min^{-1}; N_2 flow rate = 10 liters h^{-1}). (A) Fresh catalyst; (B) deactivated catalyst; (C) partially reactivated catalyst (see text).

dition that the total NH_3 uptake for the fresh catalyst corresponds to about 3 NH_3 molecules per channel intersecting element (the unit cell is conveniently divided into four equivalent intersecting elements which comprise the channel intersections (*12*) provided that there is no important contribution from other amorphous or crystalline impurity phases). In addition, 2.8 NH_3 molecules are chemisorbed under the same conditions in the γ state, which is only slightly less than the total (theoretical) number of acidic sites calculated from the Si/Al ratio and agrees well with the chemisorbed amounts measured by microcalorimetry for similar materials (see Table 2 in Ref. (*3*)).

The desorption activation energies from the α, β, and γ states are readily evaluated from TPD experiments at varying heating rates (5 to 40 K min^{-1}), assuming the desorption process to be formally of first order and using the formulation described by Redhead (*13*), Cvetanovic and Amenomiya (*14*), or Menzel (*10*). Experimental adsorption activation energies are 20.2 (84.6), 23.1 (96.7), 38.8 (162.3) kcal mol^{-1} (kJ mol^{-1}) for the α, β, and γ states, respectively. These values may be compared to heats of adsorption values ranging from 38.3 kcal mol^{-1} (160 kJ mol^{-1}) (maximum heat of adsorption) down to 24.0 kcal mol^{-1} (100 kJ mol^{-1}) (when 2.5–3.0 moles of NH_3 are adsorbed per unit cell) measured with a heat-flow microcalorimeter.

Typical extrapolation plots are shown in Fig. 6, using the relationship

$$\ln(T_p^2/\beta) = E_1/RT_p + \ln(E_1/k_1^0R) \quad (1)$$

TABLE 1

Catalytic Activity and Ammonia Adsorption of H–ZSM-5-Type Zeolite[a]

Parameter	Catalyst		
	Fresh	Deactivated[b]	Partially regenerated[c]
CH_3OH conversion[d]			
Methanol	0.0	58.1	*e*
Dimethyl ether	0.0	33.9	*e*
Hydrocarbons	98.5	6.6	*e*
NH_3 adsorption[f]			
Total uptake[g]	13.3	0.90	3.4
Physisorbed (293 K)[g]	3.4	0.54	0.6
Weakly adsorbed (α state)	3.5	0.08	0.2
Chemisorbed (β state)	3.6	—	1.6
Strongly chemisorbed (γ state)	2.8	0.28	1.0

[a] Acidic zeolite HTZ-1.

[b] Methanol-to-hydrocarbons reaction (643–648 K), P = 1 atm, WHSV = 3 h^{-1}.

[c] Following temperature rise up to 873 K under N_2 in temperature-programmed desorption experiment (see text).

[d] Product distribution as C_1 normalized (%).

[e] No catalytic data.

[f] Molecules per unit cell (UC); UC molecular weight assumed to be about 6100.

[g] Maximum value; no correction of reference concentration profile for diffusion broadening in total uptake evaluation.

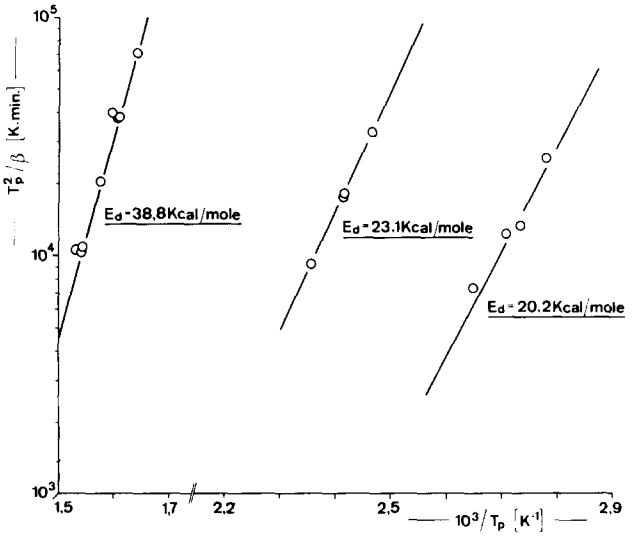

FIG. 6. First-order plots for temperature-programmed desorption of NH_3 form of protonated HTZ-1 catalyst.

in which T_p is the temperature at which the desorption curve shows a peak and β is the heating rate. k_1^0 and E_1 are the first-order preexponential term and activation energy, respectively.

DISCUSSION

In a discussion of the acidic properties of ZSM-5-type materials, it may be worth concentrating at first on the nature of the acidic hydroxyl groups which are detected by infrared spectroscopy. Barthomeuf (*11*) has recently proposed a correlation (see Fig. 2 in Ref. (*11*)) which relates the change in the (square) wavenumber ($\bar{\nu}^2$) of acidic hydroxyl groups to the (Al/(Al + Si)) ratio of the corresponding zeolite and found that the increase in $\bar{\nu}^2$ at larger Al content was largely due to an increase in the force constant of the hydroxyl band due to collective interactions between negatively charged aluminum centers in the zeolite framework. This correlation (as a function of (Al/(Si + Al))) seems however to break down at low Al content (ZSM-5 and dealuminated mordenite) and the question may be raised whether acidic hydroxyls in such materials behave differently.

The evaluation of collective properties due to field effects in zeolites of course implies that all charge interactions are considered (*15*, *16*). The interaction between lattice charges will depend not only on the density of such charges but also on their average separation. We can approach this problem conveniently by introducing a pseudo-electric-field parameter, E, defined as

$$E = \begin{pmatrix}\text{Average framework}\\ \text{Charge density}\end{pmatrix} \times \frac{1}{\text{Average distance between Al centers}} \qquad (2)$$

or

$$E = \left(\frac{\text{Al}}{\text{Al + Si}} \cdot \rho\right)^{4/3} \qquad (3)$$

ρ being the T-atoms framework density, i.e., the number of T-atoms per 1000 Å^3 (*17*). The correlation between $\bar{\nu}^2$ and E for a variety of zeolites (see Fig. 2 in Ref. (*11*) for appropriate literature references) is shown in Fig. 7, from which it is apparent that acidic hydroxyls in both

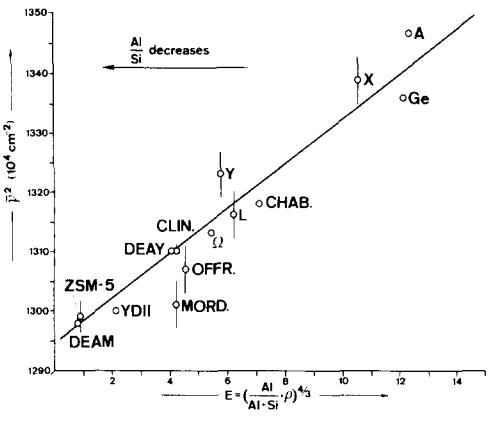

FIG. 7. Changes in the square wavenumber, $\bar{\nu}^2$, of acidic hydroxyl groups of various zeolites as a function of average internal field, E (data adapted from Ref. (*11*), see text): Ge = Ge zeolite; A = Type A; X = Type X; CHAB = chabazite; Y = Type Y; L = Type L; Ω = zeolite omega; OFFR = offretite; MORD = mordenite; CLIN = clinoptilolite; DEAY = dealuminated Y zeolite; YDII = aluminum-deficient Y zeolite; DEAM = dealuminated mordenite; ZSM-5 = protonated ZSM-5 zeolite.

dealuminated mordenite and ZSM-5 behave normally with respect to other zeolite materials and that the ir-band shift measurement is not an appropriate technique to evaluate the acid strength of highly siliceous materials (for which small variations of E and therefore $\bar{\nu}^2$ are expected, see Fig. 7). Some scattering in the ir band frequency values will of course be present in all cases due to secondary effects of counterions or a nonstatistical distribution of Al centers through the zeolite framework.

The general behavior during activation of the three ir hydroxyl bands at 3600, 3660, and 3720 cm^{-1}, respectively, agrees well with the previously reported data of Védrine *et al.* (*1*). It may be demonstrated in a more pictorial fashion by the use of difference ir spectroscopy. Namely, the progressive release of adsorbed water is more clearly evidenced while it is neatly confirmed that the band at 3600 cm^{-1} first increases and then (above 573 K) decreases upon dehydration, as compared to the 3720- to 3740-cm^{-1} band for which the intensity only decreases above 673 K. The assignments of the 3720- to 3740-cm^{-1} and 3600-cm^{-1} bands to hydrated silanol groups and Si–OH–Al groups, respectively, were discussed previously (*1*, *3*).

The ir pyridine adsorption data shown here differ from those of Védrine *et al.* (*1*) in that pyridine was adsorbed in the latter case at a given temperature on materials progressively outgassed at higher temperatures, while in the present case pyridine is progressively desorbed from a sample activated at 723 K, i.e., near the optimal activation temperature for pyridine adsorption as seen from Fig. 5 of Ref. (*1*). The faster decrease upon progressive desorption of the pyridinium ion band intensity as compared to coordinated pyridine (see Fig. 4), may be explained in two ways. In agreement with the suggestion of Auroux *et al.* (*3*), one could conclude that Lewis acidic sites are stronger than Brønsted acidic sites. Another possibility would be that the zeolite functions as an ionizing solvent (*11*) such that pyridinium ions have apparently a higher mobility than coordinated pyridine molecules. It should also be recalled that the binding modes of pyridine are drastically different in both cases: electrostatic interactions prevail for the pyridinium ion while coordinated pyridine interacts by its electron lone pair, i.e., in a configuration where it will tend to be perpendicular to the (adsorption site) surface. This would imply larger diffusion restrictions in the case of coordinated pyridine, mainly at high concentrations in Lewis sites, due to the restricted pore size of ZSM-5-type zeolites. It may be seen from Fig. 3 that the removal of pyridinium ions is accompanied by an extensive dehydration, as evidenced by the ir-band intensity decrease at 3440 cm^{-1}, while it is surprising to note little change in the coordinated pyridine ir bands (Fig. 4). A scheme such as Fig. 8 may account for these observations. The desorption of pyridinium ions

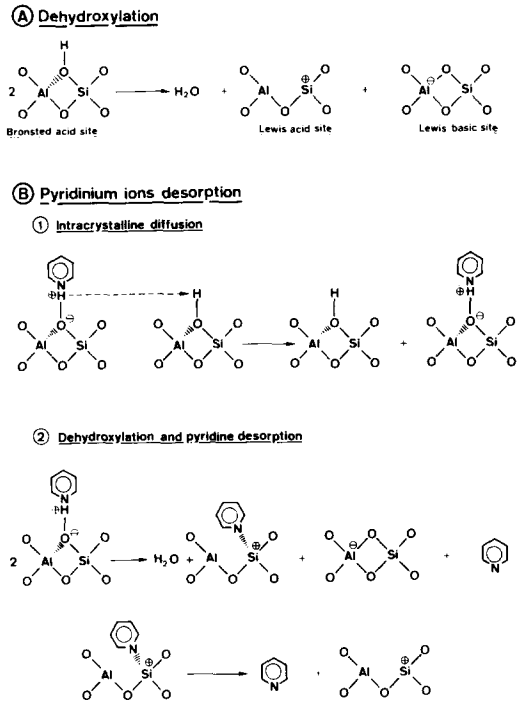

FIG. 8. Interaction of pyridine with Brønsted and Lewis acidic sites.

(Fig. 8b-2) includes diffusion steps in which pyridine jumps from one Brønsted site to another (Fig. 8b-1) and occurs in a way nearly identical to thermal dehydroxylation (Fig. 8a), which releases water. In the presence of pyridine, however, dehydroxylation seems to occur faster (probably due to the highly basic character of pyridine) and coordinated pyridine species may be formed to some extent. The latter will of course also desorb and the slower decrease in intensity of the coordinated pyridine ir band could then be explained by a near compensation in the formation and decomposition of pyridine Lewis acid site adducts. If Lewis acidic sites were much stronger than Brønsted acidic sites, one would expect an increase in the coordinated pyridine ir-band intensity when pyridinium ions are progressively decomposed. This is not the case.

The ammonia adsorption and TPD data, combined with the ir information, may be used to obtain more insight into the nature and location of the acidic sites in ZSM-5-type zeolites. Let us first consider the data for the fresh (unused) catalyst. The total amount of NH_3 irreversibly adsorbed at 293 K, i.e., about 9.9 mol per unit cell in our case (for the HTZ-zeolite), agrees well with the value of 9.76 reported by Anderson *et al.* (*4*) and the number of moles adsorbed in the γ state (which has the highest desorption activation energy), i.e., 2.8 mol, agrees with the number of strong acidic sites found in such materials by microcalorimetry (*3*). The measured activation energy (38.8 kcal mol^{-1}) for the desorption of ammonia from these sites is in excellent agreement with the maximum heat of adsorption (38.3 kcal mol^{-1}) measured by microcalorimetry (*3*). These similarities give confidence to our analysis and enable us to compare data obtained using different techniques and materials.

The γ chemisorption state may hence be associated with the adsorption of NH_3 on the strong, structural Brønsted and/or Lewis acidic sites. These are also the sites which determine the catalytic activity of the material as a 90% decrease in their number roughly corresponds to an identical decrease in the methanol conversion (see Table 1). The intensity of the γ state should then decrease upon Na exchange or when the Si/Al ratio is increased. This was actually observed by Anderson *et al.* (*4*). It may be worth adding that the relative amount of γ-state sites per unit cell is less than 4, which is perfectly compatible with the earlier proposal (*18*) that the active sites are located at the channel intersections. The rather large width of the γ-state TPD peak suggests a rather wide acidity spectrum for the strong acid sites in agreement with the microcalorimetry data (*3*).

The β-chemisorption state is observed in both H–ZSM-5 and Na–ZSM-5. It increases with Na content (Na–ZSM-5 vs H–ZSM-5) but decreases when the Si/Al ratio is increased for a protonated mate-

rial (*4*). It is characterized by a NH_3 desorption activation energy of 23.1 kcal mol^{-1} which should be compared to a heat of adsorption of 19.1–28.9 kcal mol^{-1} on Na–ZSM-5 (*3*) of 24 kcal mol^{-1} on Na–mordenite (*19*), and of 29 (*3*) or 19 (*19*) kcal mol^{-1} on the H and Na forms of Y zeolite, respectively. The β state is completely erased in a deactivated zeolite but seems to be more easily regenerated (at least partially) than the γ state. It is tempting to associate the β state with the presence of the crystallites and Na counterions which are known to act as adsorption centers for ammonia (*19–21*). The β state would then increase at the expense of the γ state upon Na exchange and would be less abundant in zeolites having lower Al content or showing larger crystallites. Organic residues blocking the β state should be rather easily removed upon regeneration (as observed) as they are most probably located on the external surface of the zeolite or in the vicinity of Na-exchanged sites.

The α-chemisorption state does not seem to depend extensively on acidification treatment (it only increases slightly) or Si/Al ratio (*4*) and it seems therefore more reasonable to assign it to sites located on the external surface or to some type of extraneous material, or to interaction of NH_3 molecules with surface oxide or hydroxyl groups by nonspecific hydrogen bonds. The corresponding low NH_3 desorption activation energy (20.2 kcal mol^{-1}) would support such an assignment.

Finally, some parallelism should be drawn between the ammonia TPD and the ir data, namely, the behavior of the β state and that of the 3720- to 3740-cm^{-1} band or that of the γ state with respect to the 3600-cm^{-1} band. The 3600-cm^{-1} band decreases with increasing Si/Al ratio and Na exchange as does the γ state (*1, 3*) and was found by ir to interact strongly with ethylene (*8*). The latter confirms the relevance of both to the characterization of the active sites. By contrast, the 3720- to 3740-cm^{-1} band is present in a nonacidified catalyst (i.e., directly after calcination of the precursor) and it increases slightly upon acidification (*3*); it does not depend extensively on the Si/Al ratio and interacts less with adsorbed ethylene and pyridine and can thus be appropriately identified with the β state and also the α state.

As conclusions, the following statements are proposed, some of which may require further clarification:

(i) infrared spectroscopy (ir) is not the best technique when used alone to characterize acidic hydroxyl groups in zeolites having a high Si/Al ratio; indeed, collective interactions play a small role in such a case and resulting hydroxyl group ir band shifts are not significant;

(ii) the ir band at 3600 cm^{-1} is characteristic of strong Brønsted sites which are also responsible (in part) for the adsorption of ammonia in the highly energetic γ state (NH_3 desorption activation energy = 38.8 kcal mol^{-1}); these active sites are located at channel intersections; they are readily dehydrated above 350 K but not easily rehydrated at room temperature possibly due to the hydrophobicity of ZSM-5-type materials; the NH_3 γ-chemisorption state also characterizes strong Lewis acidic sites;

(iii) the ir band at 3720–3740 cm^{-1} corresponds to hydroxyl groups of lower acidity which adsorb NH_3 in a less energetic β state (23.1 kcal mol^{-1}) or α state (20.2 kcal mol^{-1}); its intensity should decrease with increasing crystal size or crystallinity and decreasing amounts in aluminosilicate or siliceous impurities, which are interrelated; it is assigned to terminal silanol groups on the surface of the zeolite or impurities; these hydroxyls are most easily poisoned during hydrocarbon reactions and regenerated upon thermal treatment; note also that the β state is a likely indication of the adsorption of NH_3 on Na counterions;

(iv) the proper activation of an NH_3-containing ZSM-5 material (including NH_4–ZSM-5) must lead ultimately to desorption of NH_3 from the γ state which means that such materials much be activated at 823–873 K in order to obtain the strong acid sites;

(v) pyridinium ions readily decompose above 473 K and help in the dehydroxylation of H–ZSM-5 leading to Lewis acid sites; these ions may diffuse easily in the zeolite framework which is not surprising as zeolites are thought to behave as ionizing solvents (*11*).

ACKNOWLEDGMENTS

The authors thank Drs. H. Topsøe and P. E. Højlund Nielsen for valuable suggestions and Dr. J. Rostrup-Nielsen for his continuing interest in this work.

REFERENCES

1. Védrine, J. C., Auroux, A., Bolis, V., Dejaifve, P., Naccache, C., Wierzchowski, P., Derouane, E. G., B. Nagy, J., Gilson, J. P., Van Hooff, J. H. C., Van de Berg, J. P., and Wolthuizen, J., *J. Catal.* **59,** 248 (1979).
2. Auroux, A., Wierzchowski, P., and Gravelle, P. C., *Thermochim. Acta* **32,** 165 (1979).
3. Auroux, A., Bolis, V., Wierzchowski, P., Gravelle, P. C., and Védrine, J. C., *J. Chem. Soc. Faraday Trans. I* **75,** 2544 (1979).
4. Anderson, J. R., Foger, K., Mole, T., Rajadhyaksha, R. A., and Sanders, J. V., *J. Catal.* **58,** 114 (1979).
5. Jacobs, P. A., Uytterhoeven, J. B., Steyns, M., Froment, G., and Weitkamp, J., *in* "Proceedings, Fifth International Conference on Zeolites, Naples, Italy, June 1980," Heyden and Sons, London, 1980, p. 607.
6. Hughes, T. R., and White, H. M., *J. Phys. Chem.* **71,** 2192 (1967).
7. Ward, J. W., *J. Catal.* **9,** 225 (1967).
8. Bolis, V., Védrine, J. C., Van de Berg, J. P., Wolthuizen, J., and Derouane, E. G., *J. Chem. Soc. Faraday Trans. I* **76,** 1606 (1980).
9. Parry, E. P., *J. Catal.* **2,** 371 (1963).
10. Menzel, D., *in* "Interactions on Metal Surfaces" (R. Gomer, Ed.), pp. 101–142. Springer-Verlag, Berlin/New York, 1975.
11. Barthomeuf, D., *J. Phys. Chem.* **83,** 249 (1979).
12. Valyon, J., Mikalyfi, J., Beyer, H. K., and Jacobs, P. A., *in* "Proceedings, Workshop on Adsorption, Berlin, DDR, 1979," Vol. I, p. 134 (1979).
13. Redhead, P. A., *Vacuum* **12,** 203 (1962).
14. Cvetanovic, R. J., and Amenomiya, Y., *in* "Advances in Catalysis and Related Subjects," Vol. 17, p. 103. Academic Press, New York/London, 1967.
15. Beaumont, R., and Barthomeuf, D., *J. Catal.* **27,** 45 (1972).
16. Mikovsky, R. J., and Marshall, J. F., *J. Catal.* **44,** 170 (1976).
17. Meier, W. M., and Olson, D. H., "Atlas of Zeolite Structure Types." International Zeolite Association, 1978.
18. Dejaifve, P., Védrine, J. C., Bolis, V., and Derouane, E. G., *J. Catal.* **63,** 331 (1980).
19. Klyachko, A. L., Brueva, T. R., Mishin, I. V., Kapustin, G. I., and Rubinstein, A. M., *Acta Phys. Chem.* **24,** 183 (1978).
20. Brueva, T. R., Klyachko-Gurvich, A. L., and Rubinstein, A. M., *Izv. Akad. Nauk. SSSR Ser. Khim.*, 2807 (1972); 1254 (1974).
21. Klyachko, A. L., Brueva, T. R., Mishin, I. V., and Rubinstein, A. M., *in* "Proceedings, 4th Soviet Union Meeting on Adsorbates, Nauka, Leningrad, 1978," p. 125.
22. Argauer, R. J., and Landolt, G. R., U.S. Patent 3702 886 (1972).
23. Derouane, E. G., Dejaifve, P., B. Nagy, J., Van Hooff, J. H. C., Spekman, B. P., Naccache, C., and Védrine, J. C., *J. Catal.* **53,** 40 (1978).